



Procyanidin B1, a novel and specific inhibitor of Kv10.1 channel, suppresses the evolution of hepatoma



Wenjing Na^a, Biao Ma^a, Sai Shi^a, Yafei Chen^a, Hailin Zhang^b, Yong Zhan^a, Hailong An^{a,*}

^a Key Laboratory of Molecular Biophysics, Hebei Province, Institute of Biophysics, School of Sciences, Hebei University of Technology, Tianjin 300401, China

^b Department of Pharmacology, Hebei Medical University, Shijiazhuang 050017, China

ARTICLE INFO

Keywords:

Kv10.1 ion channel
Procyanidin B1
Liver cancer
Inhibitor
Binding pocket

ABSTRACT

Recently, we and other groups revealed that aberrant expression of Kv10.1 channel, a voltage-gated potassium ion channel, contributes to a variety of tumorigenesis process. Potent and selective inhibitor of Kv10.1 is urgently needed, both as pharmacological tools for studying the physiological functions of this enigmatic channel and as potential leads for development of anti-tumor drugs. In this study, Procyanidin B1, a natural compound extracted from the grape seed, was identified as a potent, specific inhibitor, which can inhibit the Kv10.1 channel in a concentration-dependent manner ($IC_{50} = 10.38 \pm 0.87 \mu M$), but has negligible effects on other potassium channels, including Kir2.1, HERG or KCNQ1. It was demonstrated that Procyanidin B1 directly binds to Kv10.1 channel and inhibits its currents, without increasing intracellular Ca^{2+} . Further, three amino acids, I550, T552, and Q557 in the C-linker domain of Kv10.1 were found critical for forming the binding pocket of Procyanidin B1 with Kv10.1 channel. In addition, Procyanidin B1 inhibits migration and proliferation of liver cancer cells (HuH-7 cells, HepG2 cells) through inhibiting Kv10.1, but not in Kv10.1 negatively expressed cell lines. Next, we assayed the tumor suppressing effect of Procyanidin B1 on cell line-derived xenograft mouse model. Our data showed that 15 mg/kg Procyanidin B1 can significantly suppress the growth of the tumor (HepG2) with an inhibition rate of about 60.25%. Compared with cisplatin, Procyanidin B1 has no side effect on the normal metabolism of the mice. The present work indicated that Procyanidin B1 is a promising liver cancer anti-tumor drug, and also confirmed that Kv10.1 can serve as a potential, tumor-specific drug target.

1. Introduction

Liver cancer is the fifth most common cause of cancer incidence and the third most common cause of cancer death, with an increasing trend worldwide [1,2]. Due to the poor prognosis of liver cancer, it is very important to find early tumor markers, new therapeutic targets and potential anticancer drugs for the discovery and treatment of liver cancer [3].

Kv10.1, an important voltage-gated potassium channel, also known as Eag1/KCNH1, has been confirmed that it is implicated in oncogenesis and tumor progression [4–9]. In the RNA level, Kv10.1 is mainly presented in normal brain tissue, and also expressed in a small amount in myoblasts, placenta, testis and adrenal glands [10–14]. It is noteworthy that Kv10.1 is overexpressed in approximately 70% human tumors [9,15], including liver cancer, cervical cancer, lung cancer, breast cancer, colon cancer and prostate cancer [8,11,16–19]. It has been demonstrated that Kv10.1 is predominantly expressed in the mRNA and protein levels in tissues and precancerous lesions of

cirrhosis. It has been proposed that Kv10.1 may be a potential early biomarker of liver cancer [14,16,19–22]. Moreover, inhibition of the Kv10.1 channel can reduce proliferation of several different tumor cells [11,16,18,20,23–27]. For instance, astemizole, an inhibitor of Kv10.1 channel, can decrease the proliferation and migration of cancer cells via inhibition of Kv10.1 channel activity [24,28]. Therefore, we hope to find a potent and specific inhibitor of Kv10.1 channel and explore the potential anti-hepatoma effect by targeting Kv10.1 channel.

Currently, several Kv10.1 channel inhibitors have been continually discovered. For example, several compounds including TEA⁺ (tetraethylammonium ion), Quinidin, Chloroquine (CQ) and other potassium channel inhibitor drugs can inhibit Kv10.1 channels, but lack of specificity [29–31]. Mibferdil is also an inhibitor of Kv10.1, but the dose–response of the drug has not been determined [32]. Due to the difference from Kv10.1 channel to other Kv family channels in its molecular structure that its S5-S6 linker is extended and glycosylated, peptide toxin drugs are easily affected by the sugar chains when they are bound near the hole location [33–35].

* Corresponding author.

E-mail address: hailong_an@hebut.edu.cn (H. An).

<https://doi.org/10.1016/j.bcp.2020.114089>

Received 17 February 2020; Received in revised form 21 May 2020; Accepted 8 June 2020

Available online 10 June 2020

0006-2952/ © 2020 Elsevier Inc. All rights reserved.

In recent years, natural compounds attract more and more attention because of their biosafety and the remarkable effect of treatment [36,37]. Therefore, we tried to find a natural compound drug that targets the Kv10.1 channel for tumor treatment. Procyanidin B1, one type of proanthocyanidins, is widely distributed in fruits, vegetables, nuts, seeds and so on. In particular, the seeds of grape are rich source of Procyanidin B1 without any potential genotoxic or toxicity [38]. Studies have confirmed that proanthocyanidins have a wide range of pharmacological activities, including oxidation resistance, free radical scavenging and anti-cancer activity [39–41]. However, the mechanism by which proanthocyanidins inhibit cancer is not clear.

In this study, we first showed that Procyanidin B1 can directly bind with Kv10.1 channel and inhibit its currents in a dose-dependent way. Our data also showed that the drug can suppress the proliferation and migration of liver cancer cells, and repress the growth of mouse xenograft tumors of HepG2 cells significantly through inhibition of the currents of Kv10.1. This study provides a pharmacological mechanism for elucidating the anti-tumor effect of Procyanidin B1 and demonstrates that it is a highly promising Kv10.1 channels targeted drug to brake the development of tumors.

2. Materials and methods

2.1. cDNA constructs

The plasmid encoding human Kv10.1 (GenBank accession number: NM_172362) subcloned into pEZ-M03 was synthesized by GeneCopoeia (BioProbes, USA). The Kv10.1 (I550A-T552A-Q557A) mutant was produced using Pfu DNA polymerase with a QuickChange kit (Stratagene, La Jolla, CA) and confirmed by DNA sequencing.

2.2. Cell culture and transfection

HEK293, L-O2, HuH-7 and HepG2 cells were grown, respectively, in DMEM medium, RPMI-1640 medium, DMEM medium and DMEM medium supplemented with 10% fetal calf serum and 1% penicillin/streptomycin at 37°C in a humidified 5% CO₂ atmosphere and passaged every 2 days. HEK293 cells were transfected with Kv10.1 complementary DNA (cDNA) constructs using an X-tremeGENE HP (Roche, Switzerland).

2.3. Stable expression of Kv10.1 channel in L-O2 cells, CHO cells

L-O2 cells were transfected with Kv10.1 channel complementary DNA (cDNA) constructs using an X-tremeGENE HP (Roche, Switzerland) as described previously. Twenty-four hours after the transfection, cells were trypsinised and plated on 9-cm Petri dishes in medium supplemented with 1 mg/ml geneticin G418 for 14 days. Positive colonies were selected and transferred to 24-well culture plates, and L-O2 cells stably expressing Kv10.1 were identified by western blotting and patch clamp techniques. Stably transfected L-O2 cells were cultured in RPMI-1640 medium supplemented with 10% fetal bovine serum (FBS), 600 µg/ml G418 and 1% penicillin/streptomycin. The cells were removed from the culture flask by digestion with 2.5 mg/ml trypsin (1:250) for 2 min and seeded at low density on 13-mm glass coverslips in 24-well tissue culture plates for experiments.

2.4. Rubidium efflux assay

L-O2 cells were plated at a density of 4×10^4 cells/well in poly-D-lysine-coated 96-well microplates and incubated overnight. For Rb⁺ loading, cell culture medium was aspirated, and then 200 µL of Rb⁺ loading buffer was added per well and incubated for 3 h at 37 °C, 5% CO₂. The Rb⁺ loading buffer contained (in mM): RbCl 5.4, Glucose 5, HEPES 25, NaCl 150, MgCl₂ 1, NaH₂PO₄ 0.8, CaCl₂ 2 (pH adjusted to 7.4 with NaOH). For measurement of Rb⁺ efflux block, blockers were

added to the loading buffer in the final 30 min. Following the 3 h incubation, the Rb⁺ loading buffer was removed and cells were washed gently three times with wash buffer before drug treatment. Wash buffer contained (in mM): KCl 5.4, HEPES 25, NaCl 150, MgCl₂ 1, NaH₂PO₄ 0.8, CaCl₂ 2 (pH adjusted to 7.4 with NaOH). Finally, the compound to be measured was diluted to 100 µM in the depolarizing buffer, and 200 µL of the solution was added into the 96-well plate for 10 min. Depolarizing buffer contained (in mM): KCl 90, HEPES 25, NaCl 80, MgCl₂ 1, NaH₂PO₄ 0.8, CaCl₂ 2 (pH adjusted to 7.4 with KOH). After incubation for 10 min, 150 µL supernatant was aspirated carefully into another 96-well plate, and Rb⁺ atomic absorption at 780 nm was determined with Ion Channel Reader (ICR) 8000 flame atomic absorption spectrometer (Aurora Biomed, Canada) [42]. All drugs were purchased from Chengdu DeSiTe Biological Technology Co., Ltd (Chengdu, China).

2.5. Electrophysiology

All experiments were performed at room temperature (22–25°C). Kv10.1 currents in HEK cells were recorded using the whole-cell patch clamp technique with an EPC 10 amplifier (HEKA Electronic, Germany) and PULSE software (HEKA) at an acquisition rate of 10 kHz, and signals were filtered at 2.5 kHz. The patch pipettes were made of borosilicate glass (VitalSense Scientific Instruments Company, Chengdu, China) and drawn using a P-97 puller (Sutter Instruments, Novato, USA) with a pipette resistance of 3–5 MΩ (whole-cell mode) or 1–1.5 MΩ (inside out mode) when immersed in the bath solution. Unless stated otherwise, the pipettes were filled with (in mM): KCl 130, MgCl₂ 5, EGTA 10, HEPES 10, K₂ATP 5, HEPES 10 (pH 7.4 adjusted with KOH). The standard bath solution contained (in mM): NaCl 140, KCl 4, MgCl₂ 1, CaCl₂ 1.8, HEPES 10, Glucose 10 (pH 7.4 adjusted with NaOH). Osmotic pressures fell within the ranged from 290 to 300 mOsm/l for the pipette solution and from 300 to 310 mOsm/l for the bath solution as measured by an OM815 osmometer (Löser Messtechnik, Germany). Currents were measured in the whole-cell configuration with access resistances below 3 MΩ.

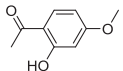
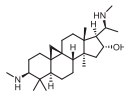
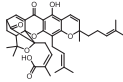
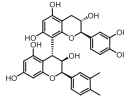
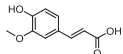
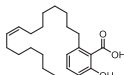
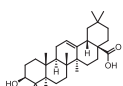
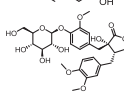
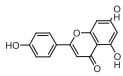
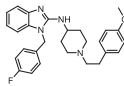
2.6. Cytoplasmic calcium measurements

L-O2 cells stably expressing Kv10.1 were seeded 24 h before measurements of cytoplasmic calcium concentrations. Cells were loaded with the fluorescent calcium indicator Fluo-3 AM (10 µM) for 30 min in dark at a 37°C incubator, and Fluo-3 AM fluorescence observations and recordings were conducted on a confocal laser scanning microscope (CLSM, SP5, Leica, Germany). Fluo-3 AM fluorescence was excited at 488 nm, and emission fluorescence was measured using a 515 nm long pass filter. Changes in [Ca²⁺]_i were represented by changes in fluorescence intensity.

2.7. Proliferation assay

Briefly, L-O2 cells, Kv10.1 stably expressed L-O2 cells, Kv10.1 knocked down HepG2 cells and normal HepG2 cells were seeded into 96-well plates (4,000–7,000 cells/per well) and cultured for 24 h, respectively. Then, the L-O2 cells were incubated for 48 h with vehicle (DMSO as the control) or Procyanidin B1 (0.1–100 µM) before the 3-(4,5-dimethylthiazol-2-yl)-2,5-diphenyltetrazolium bromide (MTT) assay. MTT solution (5 mg/mL, 20 µL) was added to each well, and the cells were incubated for 4 h. The supernatant was discarded, and DMSO (150 µL) was added to each well. The 96-well plate was placed on a shaker at 30 rounds per minute (rpm) for 10 min for the crystals to be fully dissolved. A SpectraMAX i3 (Molecular Devices, Sunnyvale, CA, USA) was used to record the absorbance at 490 nm. The percentage of viable cells after treatment with Procyanidin B1 was calculated by dividing the absorbance of the Procyanidin B1 treated group by the absorbance of the vehicle-treated group. MTT cell proliferation and cytotoxicity assay kit were purchased from Solarbio (CAS No.:298–93-1;

Table 1
Normalized Rb⁺ efflux by 9 candidate drugs (100 μM).

Natural Compound	Molecular Structure	Normalized Rb ⁺ Efflux %	Natural Compound	Molecular Structure	Normalized Rb ⁺ Efflux %
Paeonol		95.57 ± 8.32	Cyclovirobuxine		100.33 ± 4.66
Gambogic acid		97.30 ± 6.28	Procyanidin B1		82.08 ± 3.22***
Ferulic acid		93.88 ± 8.05	Ginkgolic acid		99.26 ± 4.78
Oleanolic acid		96.94 ± 3.61	Tracheloside		98.90 ± 8.54
Apigenin		103.82 ± 10.88	Astemizole		84.36 ± 3.48***

Beijing, China).

2.8. Wound healing assay

Cells were grown to 90% confluence in 24-well plates, scraped with a sterile 200 μL tip and washed twice with phosphate-buffered saline (PBS). After incubation with each own medium containing 1% fetal bovine serum following treatment with Procyanidin B1 at 0, 5, 50, or 500 μM or DMSO, the cells were photographed at 0, 24, 48 and 72 h under an inverted microscope (Olympus, Tokyo, Japan) at × 100 magnification. These experiments were carried out in quadruplication.

2.9. Molecular docking

The crystal structure of Kv10.1 revealed by cryo-EM (PDB ID: 5K7L) [33] was used as a template to construct a continuous Kv10.1 channel structure. The 5K7L structure is complemented using the model server Swiss-model [43,44]. The modeling results showed that the GMQE score was 0.71. To find the binding site of Procyanidin B1 on the Kv10.1 structure, AutoDock 4.2 [45–47] was used for molecular docking studies. AutoDock Tools v.1.5.6 [45–47] was used to prepare the PDBQT files required for receptor and ligand molecules. The acceptor (Kv10.1) structure was kept rigid, allowing the ligand to be flexible. During PDBQT file preparation, Gasteiger charges [48] were assigned to the ligand molecules. During the global docking, the entire protein is included in the grid box, and the center of the grid box coincides with the protein center. Precise docking is then performed where the drug is distributed more. The size of the grid box for precise docking is 28 Å × 32 Å × 23 Å. The center of the box was placed in the “C-linker cavity”. All other docking parameters were set to default values. We used the Lamarckian Genetic Algorithm (LGA) was used to determine the conformation of the Procyanidin B1. The times of docking were set to 100 and cluster analysis was performed to determine the optimal binding conformation of Procyanidin B1. Visualization and analysis of complexes was performed using VMD 1.9 [49] and Open-Source Pymol (<https://pymol.org>).

2.10. Xenograft experiments

Male Balb/c mice (4 weeks) purchased from Beijing Vital River Laboratory Animal Technology Co., Ltd, were used for the *in vivo* tumor growth inhibition experiments. Animals were handled according to guidelines approved by the Animal Care and Use Committee of Hebei Medical University Experimental Animal Center (license no. SCXK (Ji)

20081-003; certificate no. 909106). 8×10^6 HepG2 cells suspended in 200 μL of PBS were subcutaneously transplanted into the right flank of each mice. When the tumor volumes reached 150 mm³, mice were randomly divided into three groups (six mice per group) to be treated with control, Procyanidin B1 (15 mg/kg) or cisplatin (6.5 mg/kg) by subcutaneous injection, respectively. Mice were inspected every 2 days for tumor development, loss of body weight and general condition, and the tumor volumes were calculated using the standard formula $\text{width}^2 \times \text{length} / 2$. Relative tumor volume (RTV) was defined as the ratio of tumor volume at an indicated time versus that at the start of drug treatment. At the end of the experiment animals were euthanized by cervical dislocation. Finally, mice's tumors were dissected for comparison.

2.11. Data analysis

Graphical presentation and statistical data analysis were carried out with GraphPad Prism 7. All data were presented as mean ± SE. Statistical significance was determined using analysis of variance and the Student's *t* test. *P* values < 0.05 indicate significant difference, designated by an asterisk (*), while *P* values < 0.01 indicate very significant difference, designated using double asterisks (**). The capacitive transients of some traces in the figures were trimmed for clarity.

3. Result

3.1. Procyanidin B1 inhibits the efflux of Rb⁺ through Kv10.1

As shown in Table 1, 9 kinds of natural compounds, from traditional Chinese medicine with anti-cancer effect, were screened by the Rb⁺ efflux assay with ICR8000 in Kv10.1 stably transfected HEK-293 cells. Astemizole, the most representative Kv10.1 channel inhibitor, was adopted as the positive control (10 μM) [50]. If the candidate drug has an inhibitory effect on the Kv10.1 channel, adding the drug to the loading and depolarization process would reduce the outflow of Rb⁺, similar to the effect of astemizole. In Table 1, it was shown that 100 μM Procyanidin B1 significantly inhibits the outflow of Rb⁺. Therefore, Procyanidin B1 might has an inhibition effect on Kv10.1, which needed further confirmation.

3.2. Procyanidin B1 inhibits the currents of Kv10.1 channel in a concentration-dependent manner

Whole cell patch clamp experiment was performed to study the

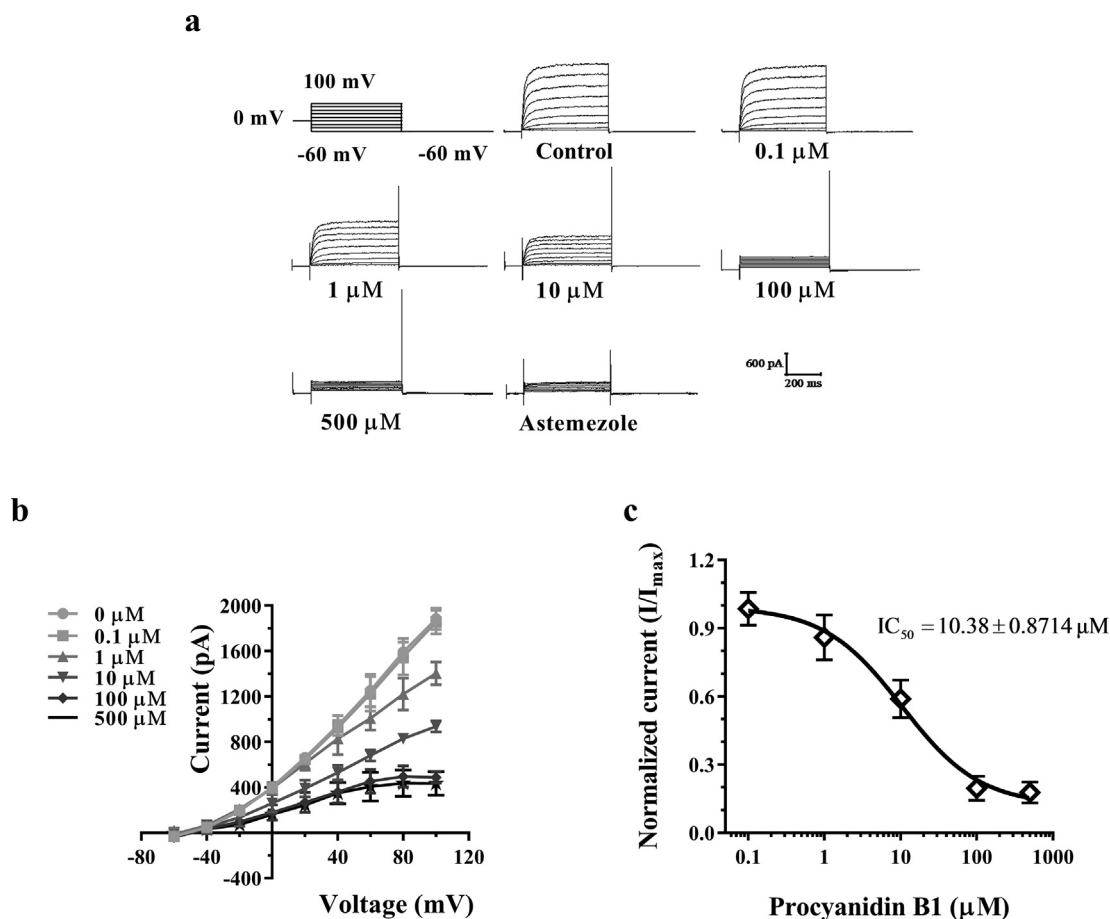


Fig. 1. Procyanidin B1 induced a dose-dependent inhibition of the Kv10.1 current in whole-cell patch experiments. (a) Representative current of Kv10.1 inhibited by various concentrations of Procyanidin B1 (0, 0.1, 1, 10, 100, 500 μM) or Astemizole (10 μM). (b) Current–voltage relationships for the experiments shown in panel (a). (c) Dose–response relationships of Procyanidin B1 on Kv10.1 currents at +100 mV. The IC_{50} of Procyanidin B1 on Kv10.1 channels is $10.38 \pm 0.87 \mu\text{M}$. Data were fitted with a Hill function ($n = 5$).

concentration dependence of Procyanidin B1 in inhibiting Kv10.1 channel. Fig. 1a shows the inhibition of Kv10.1 currents by Procyanidin B1 at various concentrations. The Kv10.1 channel current was significantly inhibited by 1 μM Procyanidin B1 and was almost completely inhibited at 100 μM . The I–V curve of Procyanidin B1 on Kv10.1 channel is shown in Fig. 1b, wherein the current of Kv10.1 decreased and the current characteristics gradually disappeared with increasing Procyanidin B1 concentrations. As shown in Fig. 1c, the dose response curve of Procyanidin B1 to Kv10.1 inhibition was shown, and the $\text{IC}_{50} = 10.38 \pm 0.87 \mu\text{M}$ at +100 mV ($n = 5$). The results showed that with the increase of Procyanidin B1 concentration, the outward and inward currents of Kv10.1 channel gradually decreased, and the overall outward rectification characteristics gradually disappeared. In conclusion, Procyanidin B1 is a small molecule inhibitor of the Kv10.1 channel, with a potent inhibitory effect on the Kv10.1 channel in a concentration-dependent manner.

3.3. Procyanidin B1 does not elevate the intracellular Ca^{2+}

Studies have shown that the Kv10.1 channel can be blocked by elevated intracellular Ca^{2+} [51,52]. In order to explore the mechanism of Procyanidin B1 inhibiting Kv10.1 channel, we measured the intracellular Ca^{2+} concentration in L-O2 cells stably expressing Kv10.1 by Fluo-3 AM fluorescence. The PBS buffer in this experiment did not include Ca^{2+} , so the change of fluorescence intensity can reflect the intracellular Ca^{2+} levels. A23187, a Ca^{2+} carrier, can carry extracellular Ca^{2+} to the cytoplasmic side of the cells and stimulates intracellular Ca^{2+} production to enhance the Fluo-3 AM fluorescence, serving as the

positive control. Unlike the Ca^{2+} carrier A23187, Procyanidin B1 did not increase $[\text{Ca}^{2+}]$, as shown in Fig. 2a. According to Fig. 2b, from the dynamic process of Ca^{2+} changes in Procyanidin B1 treated L-O2 cells stably expressing Kv10.1, it was concluded that Procyanidin B1 directly inhibits Kv10.1 channel, rather than indirect inhibiting by using Ca^{2+} as the second messenger.

3.4. The putative binding pocket of Procyanidin B1 in Kv10.1 channel

To study the putative binding site of Procyanidin B1 on the Kv10.1 channel, AutoDock4.2 was used to study the binding details [35–37]. The acceptor (Kv10.1) structure was kept rigid, allowing the ligand (Procyanidin B1) to be flexible. The times of docking was set to 100 and cluster analysis was performed to determine the optimal binding conformation of Procyanidin B1. In Fig. 3a and b, the docking simulation results show that there is an interaction between Procyanidin B1 and Ile550, Thr552 and Gln557 in the C-linker domain of the Kv10.1 channel. In addition, compared with the wild type Kv10.1, the inhibitory effect of Procyanidin B1 on the mutant Kv10.1 channel (I550A-T552A-Q557A) was significantly reduced (Fig. 3c–e, $n = 3$, $p < 0.05$). As shown in the Fig. 3f, after the mutation, the half maximal inhibitory concentration (IC_{50}) of the mutant Kv10.1 was increased by about 40 times than that of the wild type Kv10.1. These data indicate that I550, T552 and Q557 in the Kv10.1 C-linker domain form a putative binding pocket, which binds with Procyanidin B1 to inhibit Kv10.1 channel.

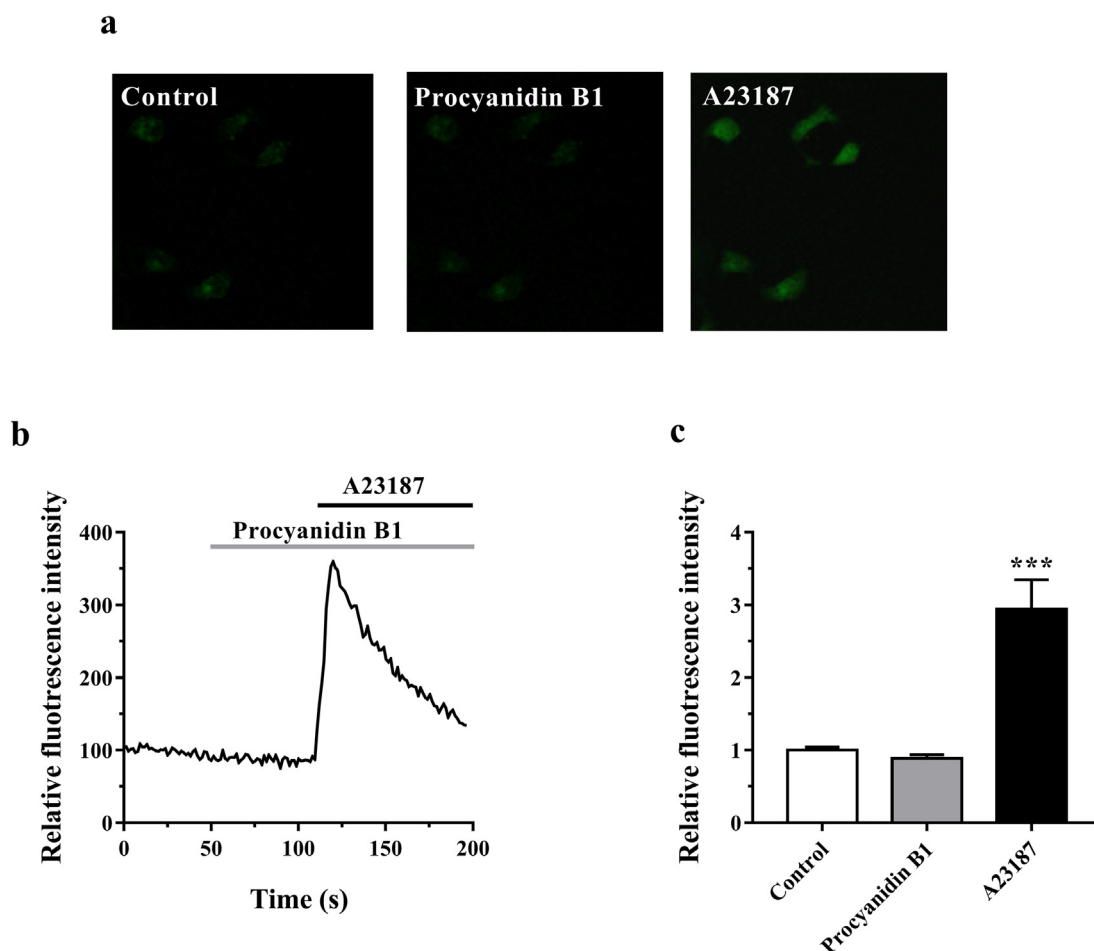


Fig. 2. Procyanidin B1 inhibits Kv10.1 channel without elevating intracellular $[Ca^{2+}]$. (a) The Fluo-3 AM fluorescence of intracellular Ca^{2+} concentrations in L-O2 cells stably expressed Kv10.1 treated with Procyanidin B1 or A23187. (b) Relative fluorescence intensity of intracellular $[Ca^{2+}]$ after sequential addition of 100 μ M Procyanidin B1 and 10 μ M A23187 to the bath solution ($n = 6$). (c) Statistical analysis of the relative fluorescence intensity in (b).

3.5. Procyanidin B1 specifically inhibits the currents of Kv10.1 channel

Since Kv10.1 is an outwardly rectified voltage-gated channel, we selected three voltage-gated potassium channels, KCNQ1 (Kv7.1) [29,53], HERG (Kv11.1) [54–57], and an inward rectification channel, Kir2.1 [58–60], as candidates for testing the specificity of Procyanidin B1 for Kv10.1. As shown in Fig. 4, the Kv10.1 channel currents were almost completely inhibited by 100 μ M Procyanidin B1. However, 100 μ M Procyanidin B1 did not significantly influence the currents of the KCNQ1/KCNE1, HERG and Kir2.1 channels. It is noteworthy that all currents can be completely suppressed by the corresponding specific inhibitors. Therefore, it can be concluded that Procyanidin B1 is a potent and specific inhibitor of Kv10.1 channel.

3.6. Procyanidin B1 suppresses tumor cell proliferation and migration by inhibiting Kv10.1

Cell viability was measured by the MTT assay in L-O2, L-O2 cells stably transfected Kv10.1 cells, and HepG2 cells, respectively. These cells were incubated for 72 h under different concentrations of Procyanidin B1. As shown in Fig. 5a, Procyanidin B1 had no influence on the proliferation of normal liver tissue cells L-O2 (a Kv10.1 negatively expressed cell line). But the proliferation of L-O2 cells which were stably transfected with Kv10.1, and HepG2 cells showed significant inhibitory effects in a concentration-dependent manner. To further demonstrate that Procyanidin B1 inhibits cell proliferation by inhibiting the Kv10.1 channel, we performed a proliferation experiment

on HepG2 cells after Kv10.1 was knocked down. Compared with NC-shRNA HepG2 cells, the inhibitory effect of Procyanidin B1 in Kv10.1-shRNA group was significantly decreased, as shown in Fig. 5b.

The effect of Procyanidin B1 on cell migration was determined by wound healing experiment in L-O2 cells, HuH-7 cells and HepG2 cells. Cells were treated with DMSO (control), 5 μ M, 10 μ M, 50 μ M, 100 μ M and 500 μ M Procyanidin B1 for 24, 48 or 72 h, respectively. As shown in Fig. 5c–e, the migration of both HuH-7 and HepG2 liver cancer cells was significantly inhibited compared to that of the normal L-O2 cells.

In conclusion, Procyanidin B1 can inhibit the proliferation and migration of liver cancer cells (HuH-7 cells, HepG2 cells) by inhibiting the Kv10.1 channel.

3.7. Procyanidin B1 inhibits the development of tumor in xenograft mice

To explore the potential anti-tumor efficacy of Procyanidin B1 *in vivo*, a subcutaneous tumor model of liver cancer (HepG2 cells) was established with Balb/c mice. Xenograft mice with HepG2 tumors were treated with different drugs through subcutaneous injection every three days. A broad-spectrum anticancer drug, cisplatin, was adopted as the control. As shown in Fig. 6b, body weight of mice treated with 6.5 mg/kg cisplatin rapidly decreased within 21 days, demonstrating that the side effect of cisplatin was quite severe. On the contrary, in Fig. 6b, body weight measurement assay showed that Procyanidin B1 had negligible side effect on the animal metabolism. As shown in Fig. 6c, d, e, both Procyanidin B1 and cisplatin can inhibit tumor development. In the tumor model treated with Procyanidin B1, it was shown in Fig. 6f

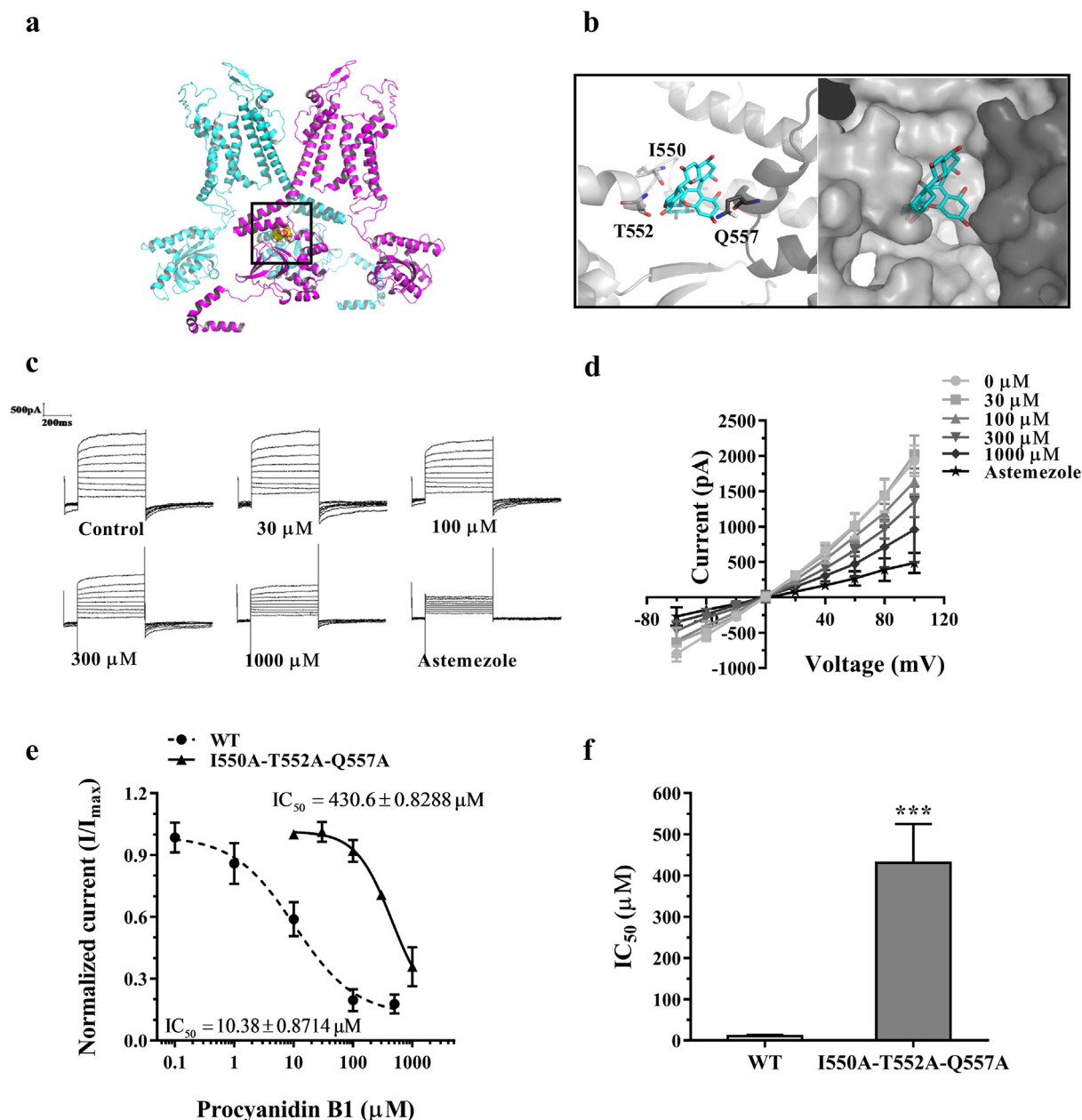


Fig. 3. Comparison of effects of different concentrations of Procyanidin B1 on wild-type Kv10.1 and mutant Kv10.1 I550A-T552A-Q557A. (a) The position where Procyanidin B1 binds with the Kv10.1 structure. To be clear, only two opposite subunits of Kv10.1 channel are shown, the protein is represented in cartoons and Procyanidin B1 is represented in spheres. (b) Molecular docking results show the putative binding pocket of Procyanidin B1 molecule to Kv10.1. (c) Characteristic Kv10.1 current induced by various concentrations of Procyanidin B1 (0, 30, 100, 300, 1000 μM or 10 μM astemizole) on I550A-T552A-Q557A Kv10.1 channels. (d) Current-voltage relationships for the experiments shown in panel (c). (e) Dose-response relationships of Procyanidin B1 on WT and I550A-T552A-Q557A Kv10.1 channel currents recorded at +100 mV. The IC_{50} of Procyanidin B1 on WT Kv10.1 channels is $10.38 \pm 0.87 \mu\text{M}$. The IC_{50} of Procyanidin B1 on I550A-T552A-Q557A Kv10.1 channels is $430.6 \pm 0.83 \mu\text{M}$. Data were fitted with a Hill function ($n = 3$). (f) Statistical analysis of IC_{50} values between WT and I550A-T552A-Q557A Kv10.1 channels.

that the tumor inhibition rate of 15 mg/kg Procyanidin B1 is about 60.25%, and that of 6.5 mg/kg cisplatin is about 76.99%. There was no significant difference in tumor suppression effect between the above two groups. From this experiment, we can conclude that Procyanidin B1 can suppress tumor development with almost no side effect in animal metabolism. The drug deserves our attention due to its high biosafety.

4. Discussion

Liver cancer is one of the malignant tumors that seriously threaten

people's health. Studies have shown that the Kv10.1 channel plays an important role in the evolution of tumors [1,2]. In this study, Procyanidin B1, a natural compound from a traditional Chinese medicine the grape seed, was identified as a potent inhibitor of the Kv10.1 channel. In addition, Procyanidin B1 can reduce cell proliferation, migration *in vitro*, and can inhibit the growth of xenograft-hepatocyte tumors *in vivo* by inhibiting Kv10.1.

As for the inhibition mechanism of Procyanidin B1, we first demonstrated that Procyanidin B1 directly inhibits the Kv10.1 channel rather than using the second messenger intracellular Ca^{2+} . In previous studies, intracellular Ca^{2+} was verified to inhibit voltage-gated

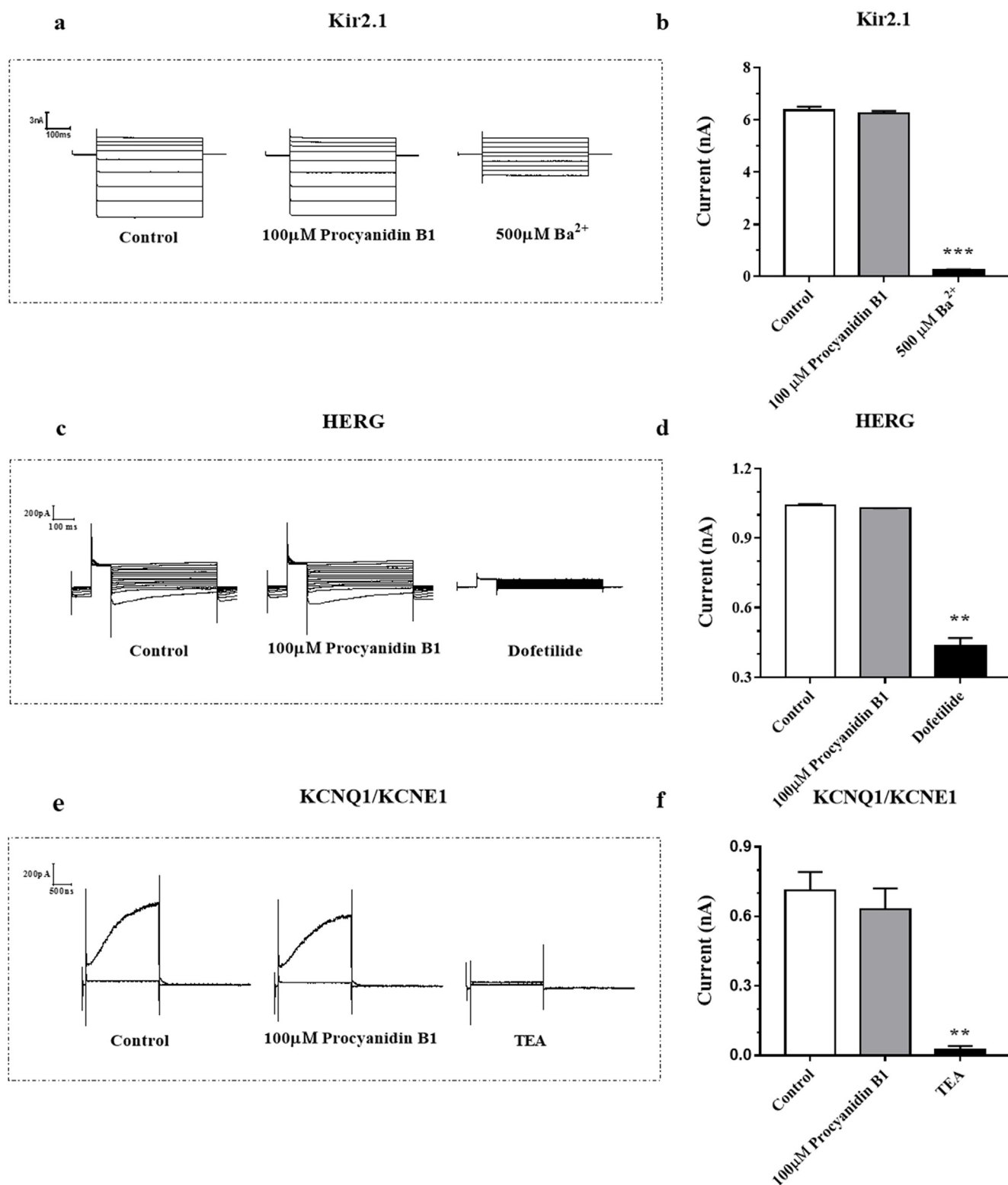


Fig. 4. Procyanidin B1 had no obviously effect for different potassium channels in whole-cell patch clamp recordings. (a, c, e) Characteristic currents of Kir2.1, HERG and KCNQ1/KCNE1 channels, respectively, in transiently transfected HEK cells, 100 μM Procyanidin B1 and the corresponding specific inhibitors subsequently. (b, d, f) The average currents of Kir2.1, HERG and KCNQ1/KCNE1 channels inhibited by 100 μM Procyanidin B1 and the corresponding specific inhibitors ($n = 4$).

potassium channels [61]. According to our experimental results, Procyanidin B1 did not cause an increasing of intracellular Ca²⁺ [62]. As shown in Fig. 3, the docking results indicated that I550, T552 and Q557 in the C-linker domain of the Kv10.1 structure form a putative binding pocket, which is critical for the direct inhibition of Procyanidin B1.

Experimental results of site-directed mutagenesis also supported this conclusion. According to the Kv10.1 gating mechanism proposed by Whicher and Jonathan R, S4 enters the cytoplasm in a hyperpolarized state to interact with and induce a rotation of the C-linker and S6 in a direction that tightens the helical bundle to close the channel [33,63].

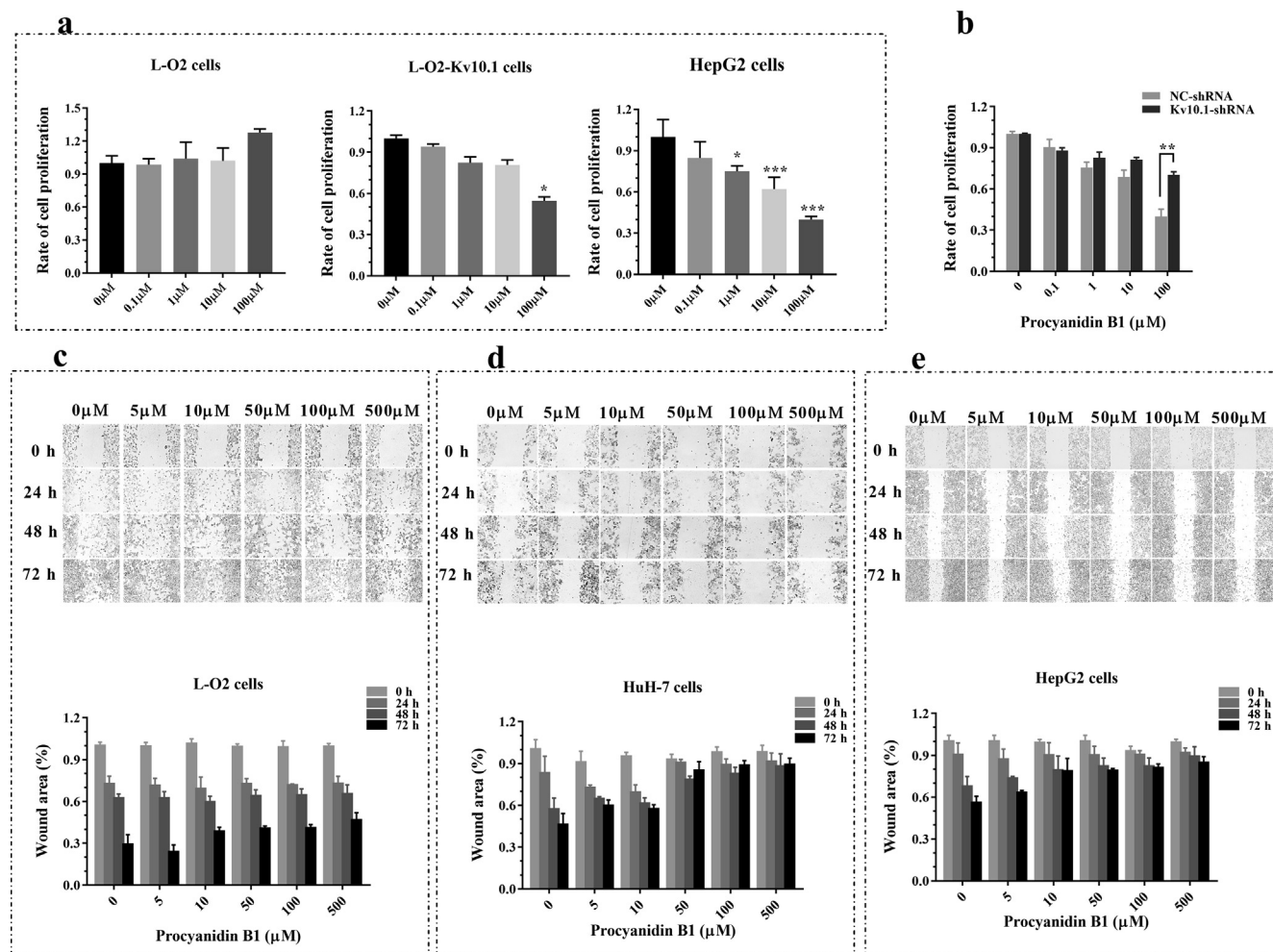


Fig. 5. Effects of various concentrations of Procyanidin B1 on the proliferation of L-O2 cells, L-O2 stably expressing Kv10.1 cells, and HepG2 cells. (a) Rate of cell proliferation of L-O2 cells, L-O2 cells stably expressing Kv10.1 cells, and HepG2 cells, treated with various concentrations of Procyanidin B1 (0, 0.1, 1, 10, 100 μ M) ($n = 12$, $*p < 0.05$, $**p < 0.01$, $***p < 0.001$, representing significant difference compared to the corresponding control cells treated with Procyanidin B1). (b) Rate of cell proliferation of HepG2 cells treated with different concentrations of Procyanidin B1 (0, 0.1, 1, 10, 100 μ M) and Kv10.1-shRNA HepG2 ($n = 6$, $*p < 0.05$, show significant difference from HepG2 cells treated by 0 μ M Procyanidin B1). (c, d, e) The wound healing assay under the condition of different concentrations Procyanidin B1 (0, 5, 10, 50, 100, 500 μ M) of L-O2 cells, HuH-7 cells and HepG2 cells ($n = 5$). (f, g, h) Rate of wound area conducted on different cell lines and different concentrations with Procyanidin B1.

The results of this study are consistent with the gating mechanism proposed by Whicher and Jonathan R. Similarly, in our group's previous study, Wang *et al.*, also found a Kv10.1 inhibitor tetrandrine, which acts on I550, T552 and Q557 in the C-linker domain of the Kv10.1 structure [64]. The binding pocket including I550, T552, Q557 might be a common inhibitor binding pocket, which needs further confirmation.

As far as we know, the precise membrane receptor of Procyanidin B1 remains unclear. Procyanidin B1 is a dimers form of Proanthocyanidins [65]. With regard to the anti-cancer effect of proanthocyanidins, Meeran, S.M. and Katiyar, S.K. showed that Proanthocyanidins inhibits the mitogenic and survival-signaling *in vitro* and tumor growth *in vivo* [66]. Mantena, S.K. and Baliga, M.S show proanthocyanidins not only can induce apoptosis, and inhibit metastasis of highly metastatic breast carcinoma cells, but it also can inhibit UV-radiation-induced oxidative stress and activation of MAPK and NF- κ B signaling in human epidermal keratinocytes to inhibit cancer. Similarly, proanthocyanidins can promote apoptosis in human epidermoid carcinoma A431 cells through caspase-3 activation via loss of mitochondrial membrane potential [39,67]. Roy, A.M. and Baliga, M.S. also find Proanthocyanidins can induce apoptosis through p53, Bax, and Caspase-3 pathways [68]. In the present work, we first discovered a

cell membrane receptor, Kv10.1, accounting for the inhibiting cancer function of Procyanidin B1.

At present, the treatment of liver cancer mainly includes surgery, radiotherapy and chemotherapy. Because liver cancer is not sensitive to radiotherapy, and the treatment of conventional chemotherapy drugs, such as adriamycin, fluorouracil, cisplatin, etc, has serious toxic and reverse effects, therefore, molecular targeted therapy attracts more and more attention [69–72]. The representative drugs are multi-target drug (sorafenib, sunitinib, and multi-kinase inhibitors) [73–75], anti-angiogenic drugs (bevacizumab) [76,77] and anti-EGFR drugs (erlotinib, cetuximab) [78,79]. They are able to significantly inhibit tumor development but with significant reverse effects, including hand-foot syndrome, diarrhea, fatigue, weakness and bleeding. Procyanidin B1, as a member of the natural compound, is not toxic to normal cells (L-O2), as can be seen in the MTT cell proliferation assay *in vitro*. Cell line derived HepG2 cells xenograft tumor shown that 15 mg/kg (100 μ M) have hardly any side effects on body weight *in vivo*. The data from *in vitro* tests and *in vivo* animal toxicity studies indicate that Procyanidin B1 are not genotoxic in nature.

Overall, the study identified a natural compound Procyanidin B1, which is a novel, selective, potent and safe Kv10.1 ion channel inhibitor and can target the Kv10.1 channel to inhibit the proliferation and

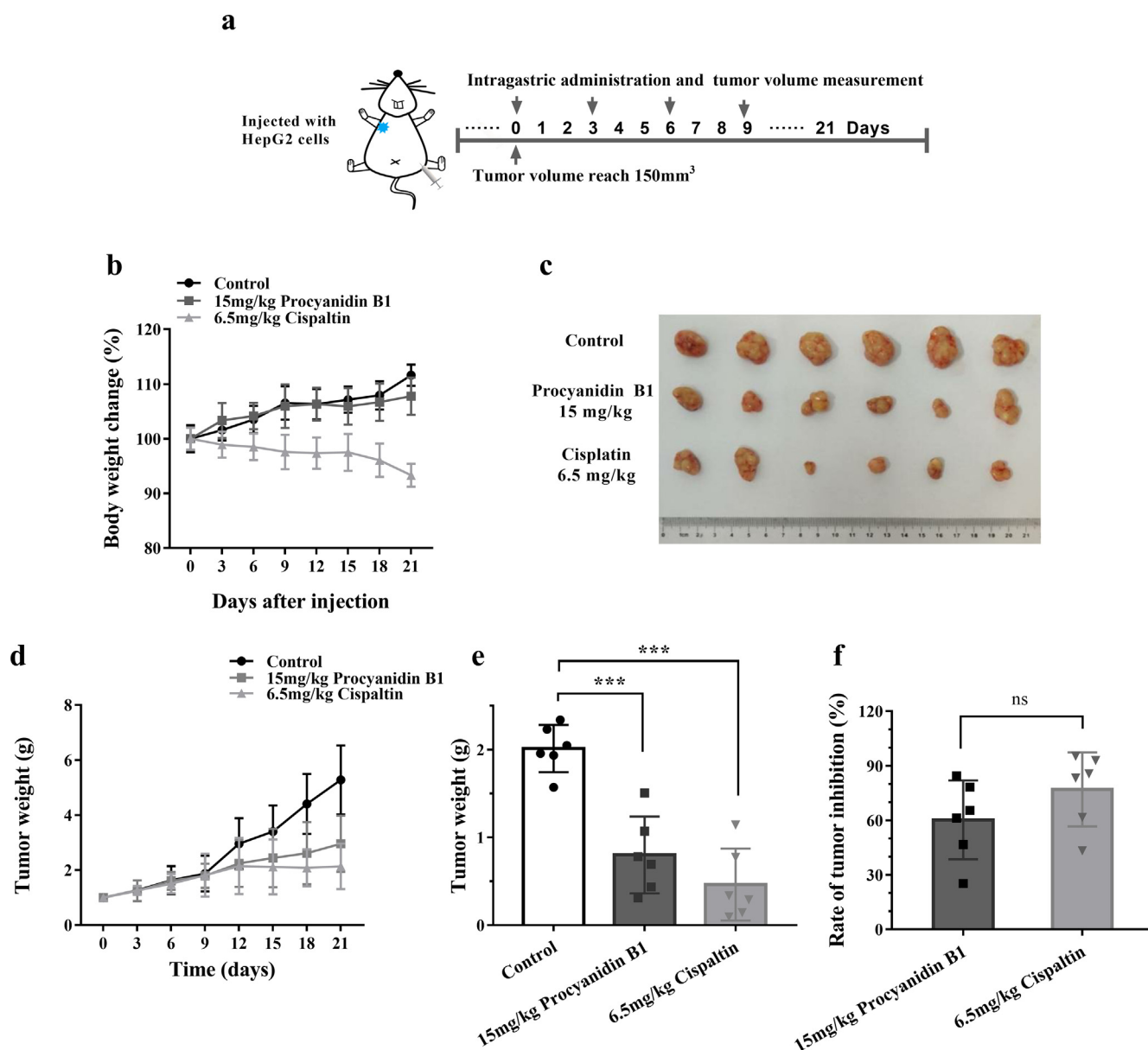


Fig. 6. Procyanidin B1 reduces tumor growth *in vivo* in a concentration-dependent manner. (a) Schematic diagram of experimental design and treatment. (b) Body weight change curve of mice treated with a vehicle control, 15 mg/kg Procyanidin B1 or 6.5 mg/kg cisplatin, respectively. (c) The tumors 21 days after Procyanidin B1 and cisplatin treatment. (d) Relative tumor volume curve of mice treated with a vehicle control, 15 mg/kg Procyanidin B1 or 6.5 mg/kg cisplatin, respectively. (e) Tumor weight of mice treated with a vehicle control, 15 mg/kg Procyanidin B1 or 6.5 mg/kg cisplatin, respectively. (f) Rate of tumor inhibition treated with a vehicle 15 mg/kg Procyanidin B1 or 6.5 mg/kg cisplatin, respectively. The calculation formula is $(C-T)/C \times 100\%$, wherein C is the average weight of the control group and T is the average tumor weight of the mice treated with various drugs.

migration of liver tumor cells, and development of xenograft-hepatocyte tumors. More importantly, the study reveals a new mechanism how Procyanidin B1 exerts inhibition effect on the Kv10.1 channel. Therefore, Procyanidin B1 has potential to be developed as a drug targeting Kv10.1 for the clinical therapy of liver cancer. It is also confirmed that Kv10.1 can be used as a target for cancer treatment.

Author contributions

Participated in research design: YZ, HA. Conducted experiments: WN, BM, SS. Performed data analysis: WN, BM and HA. Wrote or contributed to the writing of the manuscript: WN, YC, YZ and HA. Methodology and Resources: HZ, YZ, and HA.

Declaration of Competing Interest

The authors declare that they have no known competing financial interests or personal relationships that could have appeared to influence the work reported in this paper.

Acknowledgments

This work was supported by the National Natural Science Foundation of China (Grant No. 11735006 to Y Zhan, 81830061 to HL An), the Natural Science Foundation of Tianjin of China (Grant No. 19JCYBJC28300 to HL An), the Natural Science Foundation of Hebei Province of China (Grant No. C2018202302 to YF Chen), the Youth Talent Support Program of Hebei Province of China (Grant No. 2013001 to YF Chen).

References

- [1] H.B. El-Serag, K.L. Rudolph, Hepatocellular carcinoma: epidemiology and molecular carcinogenesis, *Gastroenterology* 132 (7) (2007) 2557–2576.
- [2] J.M. Llovet, A. Burroughs, J. Bruix, Hepatocellular carcinoma, *Lancet* 362 (9399) (2003) 1907–1917.
- [3] A. Forner, J.M. Llovet, J. Bruix, Hepatocellular carcinoma, *Lancet* 379 (9822) (2012) 1245–1255.
- [4] C.K. Bauer, J.R. Schwarz, Ether-a-Go-Go K⁺ channels: effective modulators of neuronal excitability, *J. Physiol.* 596 (5) (2018) 769–783.
- [5] E.D. Burg, C.V. Remillard, J.X. Yuan, Potassium channels in the regulation of pulmonary artery smooth muscle cell proliferation and apoptosis: pharmacotherapeutic implications, *Br. J. Pharmacol.* 153 (1) (2008) 99–111.
- [6] M.G. Chavez-Lopez, V. Zuniga-Garcia, J.I. Perez-Carreón, A. Avalos-Fuentes, Y. Escobar, J. Camacho, Eag1 channels as potential early-stage biomarkers of hepatocellular carcinoma, *Biologics* 10 (2016) 139–148.
- [7] N. Comes, A. Serrano-Albarras, J. Capera, C. Serrano-Novillo, E. Condom, S.R. Cajal, et al., Involvement of potassium channels in the progression of cancer to a more malignant phenotype, *BBA(BBA)-Biomembranes* 1848 (10) (2015) 2477–2492.
- [8] C.S. Ortiz, D. Montante-Montes, M. Saqui-Salces, L.M. Hinojosa, E. Hernandez-Gallegos, A. Gamboa-Dominguez, et al., Eag1 potassium channels as markers of cervical dysplasia, *Oncol. Rep.* 26 (6) (2011) 1377–1383.
- [9] H. Ouaïd-Ahidouch, A. Ahidouch, L.A. Pardo, Kv10.1 K⁺ channel: From physiology to cancer, *Eur. J. Physiol.* 468 (5) (2016) 751–762.
- [10] P. Bijlenga, T. Occhiodoro, L. Jh, C.R. Bader, L. Bernheim, J. Fischer-Lougheed, An Ether-a-Go-Go K⁺ current, Ih-Eag, contributes to the hyperpolarization of human fusion-competent myoblasts, *J. Physiol.* 512 (2) (2010) 317–323.
- [11] L. Diaz, I. Ceja-Ochoa, I. Restrepo-Angulo, F. Larrea, E. Avila-Chavez, R. Garcia-Becerra, et al., Estrogens and human papilloma virus oncogenes regulate human Ether-a-Go-Go-1 potassium channel expression, *Cancer Res.* 69 (8) (2009) 3300–3307.
- [12] B. Hemmerlein, R.M. Weseloh, F. Mello De Queiroz, H. Knotgen, A. Sanchez, M.E. Rubio, et al., Overexpression of Eag1 potassium channels in clinical tumours, *Mol. Cancer* 5 (2006) 41.
- [13] T. Occhiodoro, L. Bernheim, J.H. Liu, P. Bijlenga, M. Sinnreich, C.R. Bader, et al., Cloning of a human ether-a-go-go potassium channel expressed in myoblasts at the onset of fusion, *FEBS Lett.* 434 (1–2) (1998) 177–182.
- [14] L.A. Pardo, D. del Camino, A. Sánchez, F. Alves, A. Bruggemann, S. Beckh, et al., Oncogenic potential of Eag K⁺ channels, *EMBO J.* 18 (20) (2014) 5540–5547.
- [15] L.A. Pardo, W. Stuhmer, The roles of K⁺ channels in cancer, *Nat. Rev. Cancer* 14 (1) (2014) 39–48.
- [16] M.G. Chavez-Lopez, J.I. Perez-Carreón, V. Zuniga-Garcia, J. Diaz-Chavez, L.A. Herrera, C.H. Caro-Sanchez, et al., Astemizole-based anticancer therapy for hepatocellular carcinoma (Hcc), and Eag1 channels as potential early-stage markers of Hcc, *Tumour Biol.* 36 (8) (2015) 6149–6158.
- [17] L.M.B. Farias, D.B. Ocana, L. Diaz, F. Larrea, E. Avila-Chavez, A. Cadena, et al., Ether a go-go potassium channels as human cervical cancer markers, *Cancer Res.* 64 (19) (2004) 6996–7001.
- [18] D. Gomez-Varela, E. Zwick-Wallasch, H. Knotgen, A. Sanchez, T. Hettmann, D. Ossipov, et al., Monoclonal antibody blockade of the human Eag1 potassium channel function exerts antitumor activity, *Cancer Res.* 67 (15) (2007) 7343–7349.
- [19] J. Ousingsawat, M. Spitzner, S. Puntheeranurak, L. Terracciano, L. Trnillo, L. Bubendorf, et al., Expression of voltage-gated potassium channels in human and mouse colonic carcinoma, *Clin. Cancer Res.* 13 (3) (2007) 824–831.
- [20] L.A. Pardo, W. Stuhmer, Eag1: an emerging oncological target, *Cancer Res.* 68 (6) (2008) 1611–1613.
- [21] J.A. Rodriguez-Rasgado, I. Acuna-Macias, J. Camacho, Eag1 channels as potential cancer biomarkers, *Sensors (Basel)* 12 (5) (2012) 5986–5995.
- [22] H. Wulff, N.A. Castle, L.A. Pardo, Voltage-gated potassium channels as therapeutic targets, *Nat. Rev. Drug Discov.* 8 (12) (2009) 982–1001.
- [23] R. Garcia-Becerra, L. Diaz, J. Camacho, D. Barrere, D. Ordaz-Rosado, A. Morales, et al., Calcitriol inhibits ether-a go-go potassium channel expression and cell proliferation in human breast cancer cells, *Exp. Cell Res.* 316 (3) (2010) 433–442.
- [24] O. Gavrilova-Ruch, K. Schonherr, G. Gessner, R. Schonherr, T. Klapperstuck, W. Wohlrab, et al., Effects of imipramine on ion channels and proliferation of Igr1 melanoma cells, *J. Membr. Biol.* 188 (2) (2002) 137–149.
- [25] H. Ouaïd-Ahidouch, B.X. Le, M. Roudbaraki, R.A. Toillon, P. Delcourt, N. Prevarskaya, Changes in the K⁺ current-density of Mcf-7 cells during progression through the cell cycle: possible involvement of a H-ether. A-Gogo K⁺ channel, *Receptors Channels* 7 (5) (2001) 345.
- [26] C. Weber, F. Mello De Queiroz, B.R. Downie, A. Suckow, W. Stuhmer, L.A. Pardo, Silencing the activity and proliferative properties of the human eag1 potassium channel by rna interference, *J. Biol. Chem.* 281 (19) (2006) 13030–13037.
- [27] X. Wang, Y. Chen, H. Liu, S. Guo, Y. Hu, Y. Zhan, et al., A novel anti-cancer mechanism of nutlin-3 through downregulation of Eag1 channel and PI3k/AKT pathway, *Biochem. Biophys. Res. Commun.* 517 (3) (2019) 445–451.
- [28] B.R. Downie, A. Sanchez, H. Knotgen, C. Contreras-Jurado, M. Gynnopoulos, C. Weber, et al., Eag1 expression interferes with hypoxia homeostasis and induces angiogenesis in tumors, *J. Biol. Chem.* 283 (52) (2008) 36234–36240.
- [29] O.S. Marx, Requirement of a macromolecular signaling complex for beta adrenergic receptor modulation of the KCNQ1-KCNE1 potassium channel, *Science* 295 (5554) (2002) 496–499.
- [30] F. Gomez-Lagunas, Quinidine interaction with Shab K⁺ channels: pore block and irreversible collapse of the K⁺ conductance, *J. Physiol.* 588 (15) (2010) 2691–2706.
- [31] B. Valdes-Abadia, R. Moran-Zendejas, J.M. Rangel-Flores, A.A. Rodriguez-Menchaca, Chloroquine inhibits tumor-related Kv10.1 channel and decreases migration of Mda-Mb-231 breast cancer cells in vitro, *Eur. J. Pharmacol.* 855 (2019) 262–266.
- [32] F. Gomez-Lagunas, C. Barriga-Montoya, Mibefradil inhibition of the cole-moore shift and K⁺-conductance of the tumor-related Kv10.1 channel, *Channels (Austin)* 11 (5) (2017) 373–376.
- [33] J.R. Whichey, R. Mackinnon, Structure of the voltage-gated K⁺ channel Eag1 reveals an alternative voltage sensing mechanism, *Science* 353 (6300) (2016) 664–669.
- [34] E. Lorinczi, J.C. Gomez-Posada, P. De La Pena, A.P. Tomczak, J. Fernandez-Trillo, U. Leipscher, et al., Voltage-dependent gating of Kcnh potassium channels lacking a covalent link between voltage-sensing and pore domains, *Nat. Commun.* 6 (2015) 6672.
- [35] A.P. Tomczak, J. Fernandez-Trillo, S. Bharill, F. Papp, G. Panyi, W. Stuhmer, A. New, et al., Mechanism of voltage-dependent gating exposed by Kv10.1 channels interrupted between voltage sensor and pore, *J. Gen. Physiol.* 149 (5) (2017) 577–593.
- [36] T. Liu, X. Liu, W. Li, Tetrandrine, a Chinese plant-derived alkaloid, is a potential candidate for cancer chemotherapy, *Oncotarget* 7 (26) (2016) 40800–40815.
- [37] B.B. Mishra, V.K. Tiwari, Natural products: an evolving role in future drug discovery, *Eur. J. Med. Chem.* 46 (10) (2011) 4769–4807.
- [38] J. Yamakoshi, M. Saito, S. Kataoka, M. Kikuchi, Safety evaluation of proanthocyanidin-rich extract from grape seeds, *Food Chem. Toxicol.* 40 (5) (2002) 599–607.
- [39] S.K. Mantena, M.S. Baliga, S.K. Katiyar, Grape seed proanthocyanidins induce apoptosis and inhibit metastasis of highly metastatic breast carcinoma cells, *Carcinogenesis* 27 (8) (2006) 1682–1691.
- [40] A. Mittal, C.A. Elmets, S.K. Katiyar, Dietary feeding of proanthocyanidins from grape seeds prevents photocarcinogenesis in Skh-1 hairless mice: relationship to decreased fat and lipid peroxidation, *Carcinogenesis* 24 (8) (2003) 1379–1388.
- [41] R.P. Singh, A.K. Tyagi, S. Dhanalakshmi, R. Agarwal, C. Agarwal, Grape seed extract inhibits advanced human prostate tumor growth and angiogenesis and upregulates insulin-like growth factor binding protein-3, *Int. J. Cancer* 108 (5) (2004) 733–740.
- [42] J. Karczewski, J. Wang, S.A. Kane, L. Kiss, K.S. Koblan, J.C. Culbertson, et al., Analogs of Mk-499 are differentially affected by a mutation in the S6 domain of the herg K⁺ channel, *Biochem. Pharmacol.* 77 (10) (2009) 1602–1611.
- [43] S. Bienert, A. Waterhouse, T.A.P. De Beer, G. Tauriello, G. Studer, L. Bordoli, et al., The swiss-model repository-new features and functionality, *Nucleic Acids Res.* 45 (D1) (2017) D313–D319.
- [44] A. Waterhouse, M. Bertoni, S. Bienert, G. Studer, G. Tauriello, R. Gumienny, et al., Swiss-model: homology modelling of protein structures and complexes, *Nucleic Acids Res.* 46 (W1) (2018) W296–W303.
- [45] G.M. Morris, R. Huey, W. Lindstrom, R.K. Belew, D.S. Goodsell, et al., Autodock4 and Autodocktools4: automated docking with selective receptor flexibility, *J. Comput. Chem.* 30 (16) (2009) 2785.
- [46] F. Stefano, A.J. Olson, A force field with discrete displaceable waters and desolvation entropy for hydrated ligand docking, *J. Med. Chem.* 55 (2) (2012) 623–638.
- [47] S. Cosconati, S. Forli, F.A.L. Perryman, R. Harris, D.S. Goodsell, A.J. Olson, Virtual screening with autodock: theory and practice, *Expert Opin. Drug Discov.* 5 (6) (2010) 697–707.
- [48] J. Gasteiger, M. Marsili, Iterative partial equalization of orbital electronegativity—a rapid access to atomic charges, *Tetrahedron* 36 (22) (1980) 3219–3228.
- [49] W. Humphrey, A. Dalke, K. Schulten, Vmd: visual molecular dynamics, *J. Mol. Graph.* 14 (1) (1996) 33.
- [50] R.E. Garcia-Ferreiro, D. Kerscheneister, F. Major, F. Monje, W. Stuhmer, L.A. Pardo, Mechanism of block of Eag1 K⁺ channels by imipramine and astemizole, *J. Gen. Physiol.* 124 (4) (2004) 301–317.
- [51] R. Schohner, A.K. Born, S.H. Heinemann, Inhibition of human ether a go-go potassium channels by Ca²⁺/calmodulin, *EMBO J.* 19 (13) (2004) 3263–3271.
- [52] U. Ziechner, R. Schonherr, A.K. Born, O. Gavrilova-Ruch, R.W. Glaser, M. Malesevic, et al., Inhibition of human ether a go-go potassium channels by Ca²⁺/calmodulin binding to the cytosolic N- and C-termini, *FEBS J.* 273 (5) (2006) 1074–1086.
- [53] C. Bellocq, A.C. Van Ginneken, C.R. Bezzina, M. Alders, D. Escande, M.M.A.M. Mannens, et al., Mutation in the Kcnq1 gene leading to the short Qt-interval syndrome, *Circulation* 109 (20) (2004) 2394–2397.
- [54] M.R. Bowliby, Pen Ravi, H. Zhang, J. Dunlop, Herg (KCNH2 or Kv11.1) K⁺ channels: screening for cardiac arrhythmia risk, *Curr. Drug Metab.* 9 (9) (2008) 965–970.
- [55] E. Ficker, W. Jarolimek, J. Kiehn, A. Baumann, A.M. Brown, Molecular determinants of dofetilide block of herg K⁺ channels, *Circ. Res.* 82 (3) (1998) 386–395.
- [56] M.M. Al-Owais, N.T. Hettiarachchi, H.M. Kirtan, M.E. Hardy, J.P. Boyle, J.L. Scragg, et al., A key role for peroxynitrite-mediated inhibition of cardiac Erg (Kv11.1) K⁺ channels in carbon monoxide-induced proarrhythmic early afterdepolarizations, *FASEB J.* 31 (11) (2017) 4845–4854.
- [57] J.I. Vandenberg, M.D. Perry, M.J. Perrin, M.E. Hardy, J.P. Boyle, J.L. Scragg, et al., Herg K⁺ channels: structure, function, and clinical significance, *Physiol. Rev.* 92 (3) (2012) 1393–1478.
- [58] K.K. Bradley, J.H. Jagger, A.D. Bonev, T.J. Heppner, E.R.M. Flynn, M.T. Nelson, et al., Kir2.1 encodes the inward rectifier potassium channel in rat arterial smooth muscle cells, *J. Physiol.* 515 (3) (1999) 639–651.
- [59] J. Miale, E. Marbán, H.B. Nuss, Functional role of inward rectifier current in heart probed by Kir2.1 overexpression and dominant-negative suppression, *J. Clin. Invest.* 111 (10) (2003) 1529–1536.
- [60] B.K. Panama, A.N. Lopatin, Differential polyamine sensitivity in inwardly rectifying Kir2 potassium channels, *J. Physiol.* 571 (2) (2006) 287–302.

- [61] S.N. Wu, Y.K. Lo, H.F. Li, A.Y. Shen, Functional coupling of voltage-dependent L-type Ca^{2+} current to Ca^{2+} -activated K^{+} current in pituitary Gh3 cells, *Chin. J. Physiol.* 44 (4) (2001) 161–167.
- [62] M. Hammadi, V. Chopin, F. Matifat, M. Chasseraud, H. Sevestre, H. Ouadid-Ahidouch, Human ether a-Gogo K^{+} channel 1 (Heag1) regulates Mda-Mb-231 breast cancer cell migration through Orail-dependent calcium entry, *J. Cell Physiol.* 227 (12) (2012) 3837–3846.
- [63] J.R. Whicher, R. Mackinnon, Regulation of Eag1 gating by its intracellular domains, *Elife* 8 (2019) e49188.
- [64] X. Wang, Y. Chen, J. Li, J. Li, S. Guo, X. Lin, H. Zhang, et al., Tetrandrine, a novel inhibitor of ether-a-Go-1 (Eag1), targeted to cervical cancer development, *J. Cell Physiol.* 234 (5) (2019) 7161–7173.
- [65] P. Wang, Y. Liu, L. Zhang, W. Wang, H. Hou, Y. Zhao, et al., Functional demonstration of plant flavonoid carbocations proposed to be involved in the biosynthesis of proanthocyanidins, *Plant J.* 101 (1) (2019) 18–36.
- [66] S.M. Meeran, S.K. Katiyar, Proanthocyanidins inhibit mitogenic and survival-signaling in vitro and tumor growth in vivo, *Front. Biosci. J. Virt. Library* 13 (3) (2008) 887–897.
- [67] S.K. Mantena, S.K. Katiyar, Grape seed proanthocyanidins inhibit Uv-radiation-induced oxidative stress and activation of Mapk and Nf-Kappab signaling in human epidermal keratinocytes, *Free Rad. Biol. Med.* 40 (9) (2006) 1603–1614.
- [68] A.M. Roy, M.S. Baliga, C.A. Elmetts, S.K. Katiyar, Grape seed proanthocyanidins induce apoptosis through P53, Bax, and Caspase 3 pathways, *Neoplasia* 7 (1) (2005) 24–36.
- [69] D.L. Keefe, N. Roistacher, M.K. Pierri, Clinical cardiotoxicity of 5-fluorouracil, *J. Clin. Pharmacol.* 33 (11) (1993) 1060–1070.
- [70] E.A. Lefrak, J. Pifha, S. Rosenheim, J.A. Gottlieb, A clinicopathologic analysis of adriamycin cardiotoxicity, *Cancer* 32 (2) (1973) 302–314.
- [71] Q. Wu, S.K. Qin, F.M. Teng, C. Chen, R. Wang, Lobaplatin arrests cell cycle progression in human hepatocellular carcinoma cells, *J. Hematol. Oncol.* 3 (1) (2010) 43.
- [72] D.S. Palappallil, B.L. Nair, K.L. Jayakumar, R.T. Puvathalil, Comparative study of the toxicity of 5-fluorouracil-adriamycin-cyclophosphamide versus adriamycin-cyclophosphamide followed by paclitaxel in carcinoma breast, *Indian J. Cancer* 48 (1) (2011) 68–73.
- [73] C.H. Hsu, Y.C. Shen, Y.Y. Shao, C. Hsu, A.L. Cheng, Sorafenib in advanced hepatocellular carcinoma: current status and future perspectives, *J. Hepatocellular Carcinoma* 1 (2014) 85–99.
- [74] M. Pinter, W. Sieghart, I. Graziadei, W. Vogel, A. Maieron, R. Konigsberg, et al., Sorafenib in unresectable hepatocellular carcinoma from mild to advanced stage liver cirrhosis, *Oncologist* 14 (1) (2009) 70–76.
- [75] J.H. Shim, J.W. Park, J.I. Choi, B.J. Park, C.M. Kim, Practical efficacy of sorafenib monotherapy for advanced hepatocellular carcinoma patients in a hepatitis B virus-endemic area, *J. Cancer Res. Clin. Oncol.* 135 (4) (2009) 617–625.
- [76] A.B. Siegel, E.I. Cohen, A. Ocean, D. Lehrer, A. Goldenberg, J.J. Knox, et al., Phase II trial evaluating the clinical and biologic effects of bevacizumab in unresectable hepatocellular carcinoma, *J. Clin. Oncol.* 26 (18) (2008) 2992–2998.
- [77] V. Boige, D. Malka, A. Bourredjem, C. Dromain, C. Baey, N. Jacques, et al., Efficacy, safety, and biomarkers of single-agent bevacizumab therapy in patients with advanced hepatocellular carcinoma, *Oncologist* 17 (8) (2012) 1063–1072.
- [78] M.B. Thomas, R. Chadha, K. Glover, X. Wang, J. Morris, T. Brown, et al., Phase 2 study of erlotinib in patients with unresectable hepatocellular carcinoma, *Cancer* 110 (5) (2007) 1059–1067.
- [79] A.X. Zhu, K. Stuart, L.S. Blaszkowsky, A. Muzikansky, D.P. Reitberg, J.W. Clark, et al., Phase 2 study of cetuximab in patients with advanced hepatocellular carcinoma, *Cancer* 110 (3) (2007) 581–589.